Hindawi Publishing Corporation
Mathematical Problems in Engineering
Volume 2016, Article ID 3240720, 12 pages
http://dx.doi.org/10.1155/2016/3240720

Research Article

Application of the Value Optimization Model of Key Factors Based on DSEM

Chao Su and Zhiming Ren

College of Water Conservancy and Hydropower Engineering, Hohai University, Nanjing 210098, China

Correspondence should be addressed to Zhiming Ren; renzhiming1101@outlook.com

Received 14 March 2016; Accepted 7 June 2016

Academic Editor: Ivan Kyrchei

The key factors of the damping solvent extraction method (DSEM) for the analysis of the unbounded medium are the size of bounded domain, the artificial damping ratio, and the finite element mesh density. To control the simulation accuracy and computational efficiency of the soil-structure interaction, this study establishes a value optimization model of key factors that is composed of the design variables, the objective function, and the constraint function system. Then the optimum solutions of key factors are obtained by the optimization model. According to some comparisons of the results provided by the different initial conditions, the value optimization model of key factors is feasible to govern the simulation accuracy and computational efficiency and to analyze the practical unbounded medium-structure interaction.

1. Introduction

The rationality of numerical simulation in seismic loads plays an important role in the dynamic response analysis of the soil-structure interaction. With the development of science and technology, the research and application into the soil-structure interaction are of interest to those in the engineering profession and academia. Moreover, many researches on the unbounded media-structure interaction improve the rationality and accuracy of the foundations in frequency and time domains.

The methods for analyzing the soil-structure interaction are currently the artificial boundary method, the boundary element method, and the damping solvent extraction method. The artificial boundary method [1, 2] intercepts the bounded domain and increases the energy transfer system at the outer boundary (such as by a damper or spring-damper). But this method is not appropriate for analyzing an irregular foundation. The boundary element method [3] proposes the principle of wave amplitude attenuation of various frequencies far afield and makes a transformation into the time domain. Likewise, this method has a low computational efficiency and does not analyze a complicated unbounded media. However, through introducing and extracting the artificial damping ratio of the bounded medium, the damping solvent extraction method [4, 5] is appropriate for the simulation of the various foundations. Meanwhile, the DSEM implements the mutual conversion in the frequency-time domain and eliminates the convolution operation in the time domain.

Since the DSEM was first presented by Wolf and Song in 1994, some researches have presented gradually the perfect basis theory, the improved computational procedure, and the evaluation of key factors of the soil-structure interaction. In the computational algorithm, a series of calculation procedures had been suggested to improve the accuracy, such as the acceleration input stagger method [6], the precise step-by-step time integration scheme [7], and the subregional explicit implicit recursive method [8, 9]. In its practical application, the DSEM was applied to analyze the soil-structure interaction with fractional order [10], the nonlinear overload of the unbounded medium-arch dam [11], the impact of pile driving vibration on seawall [12], and fluid-structure dynamic interaction [13]. In the evaluation of key factors, the causes of the error of the DSEM had been analyzed and described in detail in [14–16]. Simultaneously, the key factors estimated in [17–19] have a great influence on the accuracy of the soil-structure interaction.

The size of bounded domain and the finite element mesh density were randomly assigned and the artificial damping ratio was limited in a specified scope, so the key influence factors of the DSEM were roughly analyzed both in the analysis and in the application. To meet the requirements of practical engineering and get the optimum solution of key factors, this study analyzes the dimensionless dynamic stiffness coefficients of various mediums and proposes the value optimization model of key factors. The initial conditions of the optimization model are the maximum of the difference function of the dynamic stiffness coefficient, the wave amplitude attenuation, and the maximum finite element number. Numerical verification demonstrates that the value optimization model of key factors can regulate the simulation accuracy and computational efficiency and analyze the practical infinite foundation-structure interaction.

2. Damping Solvent Extraction Method

The damping solvent extraction method is simply reviewed in this chapter. A bounded domain of the infinite media adjacent to the soil-structure interface is discretized with a finite element meshes shown in Figure 1.

2.1. Implementation in the Frequency Domain. The procedure of the DSEM consists of the following steps for each frequency, which calculate the dynamic stiffness coefficients of the unbounded medium.

Step 1. In the selected bounded domain idealized as an assemblage of the finite elements, the artificial damping ratio in the domain and the viscous dashpots at the outer boundary serve to attenuate the vibration amplitudes of the outgoing wave and reflected wave. The coefficients of the viscous dashpots per unit surface area at the outer boundary are ρc_s^* in the perpendicular direction and ρc_p^* in the tangential direction. The shear-wave velocity and the dilatation-wave velocity are affected by the factor $1 + 2i\zeta$. Consider

$$c_s^* = c_s\sqrt{1+2i\zeta}, \quad c_p^* = c_p\sqrt{1+2i\zeta}, \tag{1a}$$

$$G^* = G(1+2i\zeta), \quad a_0^* = a_0\sqrt{1+2i\zeta}, \tag{1b}$$

where G and a_0 are the shear modulus and dimensionless frequency, respectively.

Step 2. Eliminating all degrees of freedom, which are located in the medium except the interface, the dynamic stiffness condensed matrix of the bounded medium, $\widetilde{S}^f(\omega)$, is transformed from the dynamic stiffness matrix $S^f(\omega)$. The dynamic stiffness matrix of the damped bounded foundation is expresses as follows:

$$S^f(\omega) = G^* S^f(a_0^*) = G^*\left(-a_0^{*2}\overline{M}^f + ia_0^*\overline{C}^f + \overline{K}^f\right), \tag{2}$$

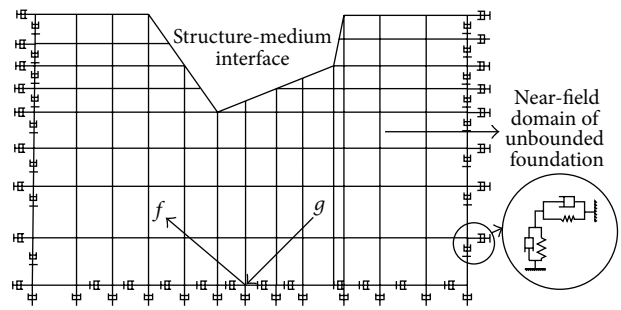

Figure 1: Finite element mesh of bounded domain adjacent to structure.

where $\overline{M}^f$, $\overline{C}^f$, and $\overline{K}^f$ are the dimensionless stiffness, damping, and mass matrices.

Step 3. Since the dynamic stiffness coefficient is derived with ω and the dynamic stiffness condensed matrix of the bounded medium, $\widetilde{S}^f(\omega)$, convert to the dynamic stiffness condensed matrix of the unbounded media, $\widetilde{S}^\infty(\omega)$, the dimensionless dynamic stiffness condensed matrix, $\widetilde{S}^\infty(a_0^*)$, is written as follows:

$$\widetilde{S}^\infty(a_0^*) = \widetilde{S}^f(a_0^*), \quad \widetilde{S}^\infty(a_0^*)_{,a_0^*} = \widetilde{S}^f(a_0^*)_{,a_0^*}. \tag{3}$$

Taking the first-order Taylor expansion of $\widetilde{S}^\infty(a_0^*)$, the dynamic stiffness matrix of the undamped unbounded medium is equal to

$$\widetilde{S}^\infty(a_0) = \widetilde{S}^\infty(a_0^*) + \widetilde{S}^\infty(a_0^*)_{,a_0^*}(a_0 - a_0^*). \tag{4}$$

2.2. Implementation in the Time Domain. The medium-structure interaction force is obtained by the DSEM in the time domain, so the motion equation of the damped bounded medium takes the form

$$\begin{bmatrix} M_{mm} & 0 \\ 0 & M_{mm} \end{bmatrix}\begin{Bmatrix} \ddot{u}_m \\ \ddot{u}_b \end{Bmatrix} + \begin{bmatrix} C_{mm} & C_{mb} \\ C_{bm} & C_{bb}^f \end{bmatrix}\begin{Bmatrix} \dot{u}_m \\ \dot{u}_b \end{Bmatrix} + \begin{bmatrix} M_{mm} & M_{mb} \\ M_{bm} & M_{bb} \end{bmatrix}\begin{Bmatrix} u_m \\ u_b \end{Bmatrix} = \begin{Bmatrix} 0 \\ R_b(t) \end{Bmatrix} \tag{5}$$

with

$$[K] = \left[\overline{K}\right] + \zeta^2\left[\overline{M}\right], \quad [C] = \left[\overline{C}\right] + 2\zeta\left[\overline{M}\right], \quad [M] = \left[\overline{M}\right], \tag{6}$$

where $[\overline{M}]$, $[\overline{C}]$, and $[\overline{K}]$ are the mass, damping, and stiffness matrices, respectively, and $\{R_b\}$ is the interaction force at the soil-structure interface. The subscript b denotes the nodes of the bounded medium at the soil-structure interface and m

denotes the remaining nodes. Furthermore, the interaction force of the soil-structure was written in [19]:

$$R_b(t) = M_{bb}\ddot{u}_b + (K_{bb} - \zeta C_{bb})u_b + K_{bm}u_m + \zeta K_{bb}v_m, \quad (7)$$

where $\ddot{u}_b$, $\dot{u}_b$, and u_b are the displacement, velocity, and acceleration vectors and the unknown u_m and v_m vectors are provided by the following equations:

$$\begin{aligned} &M_{mm}\ddot{u}_m + C_{mm}\dot{u}_m + K_{mm}u_m = -K_{mb}u_b - C_{mb}\dot{u}_b, \\ &M_{mm}\ddot{v}_m + C_{mm}\dot{v}_m + K_{mm}v_m \\ &\quad = 2M_{mm}\dot{u}_m + C_{mm}u_m + C_{mb}u_b. \end{aligned} \quad (8)$$

3. Constraint Function

The constraint functions regarded as the essential components are crucial if one wishes to solve the optimization model. Therefore, the references and analysis of the constraint functions are described in detail in this chapter.

3.1. Constraint Function of Artificial Damping Ratio. The dynamic stiffness coefficient $S^{\infty}(a_0)$ and the dimensionless dynamic stiffness coefficient $\overline{S}^{\infty}(a_0)$ of the undamped unbounded medium are, respectively, given by

$$S^{\infty}(a_0) = K^{\infty}(k(a_0) + ia_0c(a_0)), \quad (9)$$

$$\overline{S}^{\infty}(a_0) = \frac{S^{\infty}(a_0)}{K^{\infty}} = \sqrt{1-a_0^2} = k(a_0) + ia_0c(a_0). \quad (10)$$

If $a_0 \le 1$, $k(a_0) = \sqrt{1-a_0^2}$ and $c(a_0) = 0$.

If $a_0 > 1$, $k(a_0) = 0$ and $c(a_0) = \sqrt{1-(1/a_0^2)}$.

On the basis of the plural damping coefficient correspondence principle, the dimensionless dynamic stiffness coefficient of the damped unbounded medium is deduced as

$$\overline{S}^{\infty}(a_0^*) = \sqrt{1-(a_0^*)^2} \quad (11)$$

with

$$a_0^* = \frac{(\omega - i\zeta)b}{c_1} = a_0 - i\overline{\zeta}, \quad (12)$$

where a_0^* and a_0 are the dimensionless frequencies of the damped and undamped bounded medium.

The dimensionless dynamic stiffness of the damped bounded medium is determined by the size of the bounded domain, l/b, and the artificial damping ratio $\overline{\zeta}$:

$$\overline{S}(a_0^*) = \sqrt{1-(a_0^*)^2}\,\frac{1-c_1/c_2}{1+c_1/c_2}, \quad (13)$$

where c_1 and c_2 are the vibration amplitudes of the incoming wave and outgoing wave.

The dynamic stiffness coefficient of the undamped unbounded medium is calculated by taking the first-order Taylor expansion to eliminate the artificial damping ratio:

$$\overline{S}^{\infty}(a_0) = \overline{S}(a_0^*) + \overline{S}(a_0^*)_{,a_0^*}(a_0 - a_0^*). \quad (14)$$

Table 1: Values of bounded domain size and artificial damping ratio.

Case	C1	C2	C3	C4	C5	C6	C7	C8
l/b	3	3	3	3	1	3	5	7
$\overline{\zeta}$	0.01	0.1	0.5	1	0.3	0.3	0.3	0.3

The various values of the size of the bounded medium and the artificial damping ratio listed in Table 1 are used to analyze the dynamic stiffness coefficients of the undamped unbounded, damped unbounded, damped bounded, and simulating undamped unbounded medium.

When the dynamic stiffness coefficient of the undamped unbounded medium is regarded as the accurate solution, the dynamic stiffness coefficients determined by ($l/b = 3$, $\overline{\zeta} = 0.2$) shown in Figure 2 indicate that (1) the larger artificial damping ratio increases the difference between the dynamic stiffness coefficient of the undamped and damped unbounded medium; (2) the larger size of the bounded medium reduces the amplitude of the dynamic stiffness coefficient of the damped unbounded medium; (3) the smaller artificial damping ratio and the larger size of the bounded medium lead to the more accurate dynamic stiffness coefficient of the undamped unbounded medium. Therefore, the constraint function of artificial damping ratio is the difference function between the dimensionless dynamic stiffness coefficient of the undamped and damped unbounded medium.

3.2. Constraint Function of Size of the Bounded Medium. Suppose that the artificial damping ratio $\overline{\zeta} = \zeta(b/c_s)$ is zero and the size of bounded medium is l/b; e^{-iwl/c_s} is the phase angle caused by radiating the shear wave from the interface to the outer boundary of the undamped bounded domain. If the artificial damping ratio is nonzero, the frequency ω is replaced by $w - i\zeta$ and the phase angle is replaced by $e^{-\zeta l/c_1} \cdot e^{-iwl/c_1}$. Thus, $e^{-\zeta l/c_1}$ is the attenuation of the wave amplitude in the damped bounded domain.

Due to the addition of the artificial damping ratio into the bounded medium, the wave is reflected by the outer boundary and radiated to the interface. The wave amplitude attenuation function of the initial displacement wave excited at the interface is written as

$$\phi\left(\zeta, \frac{l}{b}\right) = \exp\left(-2\zeta\frac{l}{b}\frac{b}{c_1}\right) = \exp\left(-2\overline{\zeta}\frac{l}{c_1}\right). \quad (15)$$

If the wave amplitude attenuation at the interface is known, the constraint function of the size of bounded medium is transformed from function (15). Consider

$$\frac{l}{b} = -\frac{\ln(\phi_0)}{2\overline{\zeta}}. \quad (16)$$

3.3. Constraint Function of Finite Element Mesh Density. In the finite element discretization of the bounded medium, the finite element mesh of only one row, denoted as the "base row," is merely required. S_r denotes the dynamic stiffness matrix of one row of the finite element mesh with length

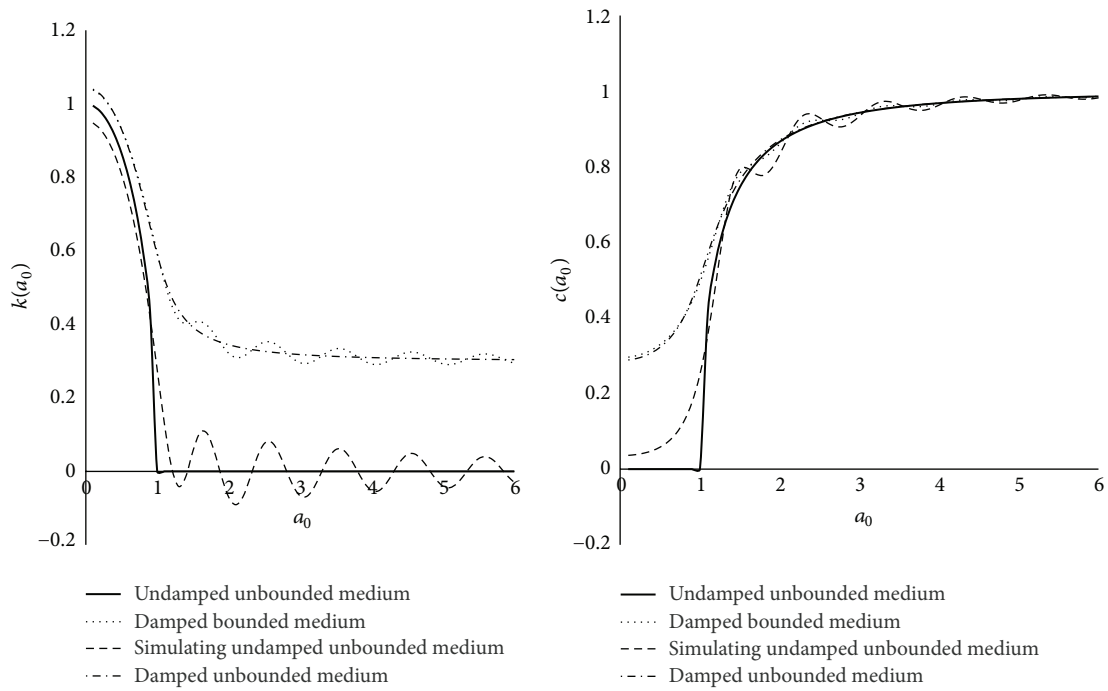

Figure 2: Dimensionless dynamic stiffness coefficients of $l/b = 3$, $\bar{\zeta} = 0.2$.

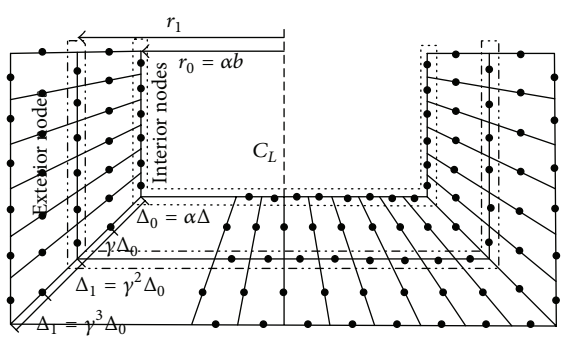

Figure 3: First row of finite element mesh.

r (Figure 3). The same is true for the condensed matrix obtained by eliminating all degrees of freedom except those related to interior nodes:

$$S_{\alpha b}(\omega) = S_b(\alpha\omega),$$
$$\widetilde{S}_{\alpha b}(\omega) = \widetilde{S}_b(\alpha\omega). \tag{17}$$

The formula relates $\widetilde{S}_{r_1}$ for exterior nodes to the corresponding matrix of interior nodes $\widetilde{S}_{r_0}$:

$$\widetilde{S}_{r_1}(\omega) = \widetilde{S}_{r_0}(\kappa\omega), \tag{18}$$

in which $\kappa = r_1/r_0 = \gamma^2$.

The dashpots are assigned at the exterior nodes of the base row. Both $\widetilde{S}_{r_0}(\gamma^{2n-2}\omega)$ and $\widetilde{S}_{r_1}(\gamma^{2n-4}\omega)$ are calculated by (18). After removing the dashpots, either $\widetilde{S}_{r_0}(\gamma^{2n-2}\omega)$ or $\widetilde{S}_{r_1}(\gamma^{2n-4}\omega)$ is assembled at the exterior nodes of the base row for frequency $\gamma^{2n-4}\omega$. $\widetilde{S}_{r_0}(\gamma^{2n-4}\omega)$ is calculated by condensing again into the dynamic stiffness matrix for interior nodes. $\widetilde{S}^f(\omega)$ is obtained by repeating the last process $n-2$ and the proportionality factor γ must satisfy

$$\frac{r_0 + 1/\sqrt{2}(\Delta + \gamma\Delta)}{r_0} = \gamma^2. \tag{19}$$

4. Value Optimization Model of Key Factors

A value optimization model of key factors is proposed to control the simulation accuracy and computational efficiency of the infinite soil-structure interaction. Then the optimum solutions of key factors of the DSEM are obtained by the value optimization.

4.1. Design Variable. Because the optimum values of key factors are provided by solving the value optimization model, the design variables of optimization model include the size of the bounded medium, the artificial damping ratio, the mesh size of finite element, and the proportionality factor.

4.2. Objective Function. The relationship between the size of bounded medium and the finite element mesh density is expressed as

$$\frac{l}{b} = \frac{\sqrt{2}}{2}\frac{\Delta}{b}\frac{1-\gamma^{2n}}{1-\gamma}. \tag{20}$$

Substituting (19) into (20), the objective function is transformed from (20).

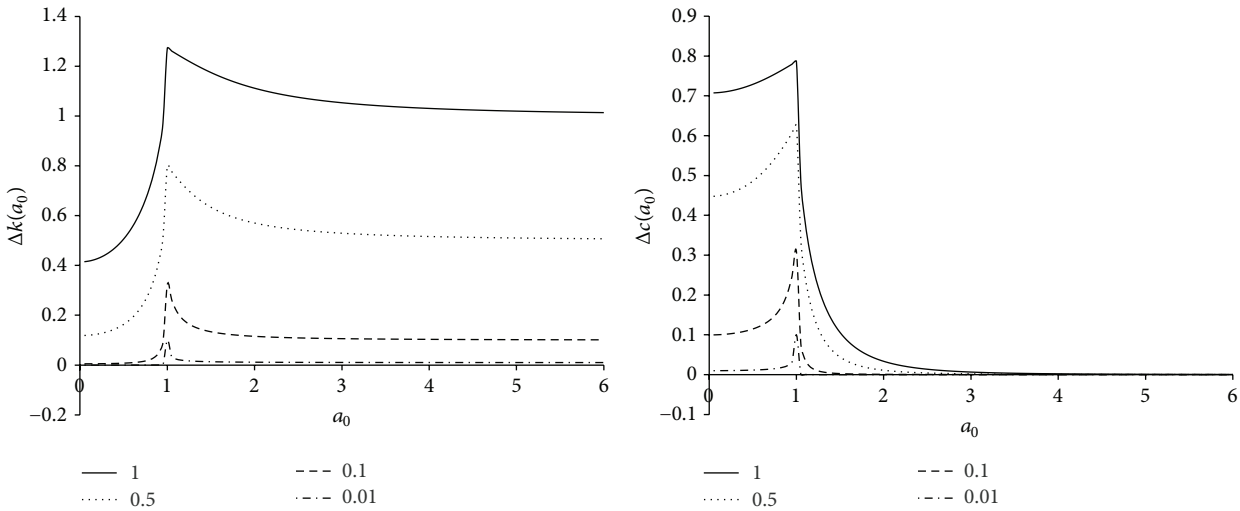

Figure 4: Difference function of dimensionless dynamic stiffness coefficients.

4.3. Constraint Function. The constraint function system is composed of the constraint functions of the size of the bounded medium, the artificial damping ratio, and the finite element mesh density as described in Section 2.

The difference function between the dimensionless dynamic stiffness coefficient of the damped and undamped unbounded foundation is expressed as follows:

$$\begin{aligned}\Delta S(a_0) &= \overline{S}^{\infty}(a_0^*) - \overline{S}^{\infty}(a_0) \\ &= \sqrt{1-(a_0^*)^2} - \sqrt{1-(a_0)^2}.\end{aligned} \tag{21}$$

The results shown in Figure 4 indicate that the smaller artificial damping ratio results in the smaller difference of the dynamic stiffness coefficient and the maximum of the difference function is calculated at the point given by $a_0 = 1$ ($\operatorname{Max} S = \Delta S(1)$).

Taking the accuracy and computational cost of the soil-structure interaction into account, the initial conditions of the optimization model consist of the maximum of the difference function of the dynamic stiffness coefficient, the wave amplitude attenuation, and the maximum finite element number in the bounded medium. Therefore, the value optimization model of key factors based on the DSEM is expressed as follows:

(1) Initial conditions: $\operatorname{Max} S$, ϕ_0, $\operatorname{Max} N$.

(2) Design variables: $\overline{\zeta}$, l/b, Δ/b, γ.

(3) Objective function:

$$\gamma = \exp\left(\frac{1}{2n}\ln\left(\frac{l}{b}-1\right)\right). \tag{22}$$

(4) Constraint functions:

$$\begin{gathered}\operatorname{abs}\left(\Delta S\left(1,\overline{\zeta}\right)\right) \le \operatorname{Max} S = \Delta S(1), \\ \frac{l}{b} = -\frac{\ln(\phi_0)}{2\overline{\zeta}}, \\ 1 + \frac{1}{\sqrt{2}b(\Delta+\gamma\Delta)} = \gamma^2, \\ n \le \operatorname{Max} N.\end{gathered} \tag{23}$$

5. Numerical Verification

5.1. Verification in the Frequency Domain

5.1.1. Problem Chosen. A cross section shown in Figure 5 is the intercepted plane of a rectangular rigid strip foundation of width $2b$ and depth b embedded in a homogeneous half plane with shear modulus G, Poisson ratio ν, and artificial damping ratio ζ. The DOFs, vertical (V), horizontal (H), and rocking (R), describe the plane motion of the foundation. The procedure analyzes the dynamic stiffness matrix, $S^{\infty}(a_0)$, of the rigid strip on the damped unbounded medium in the frequency domain.

Let P_n and Δ_n, $n \in (\mathrm{V}, \mathrm{H}, \mathrm{R})$, respectively, denote the amplitudes of the harmonic force and displacement; the vectors are related by the dynamic stiffness matrix:

$$\begin{aligned}\begin{bmatrix} P_{\mathrm{V}} \\ P_{\mathrm{H}} \\ \dfrac{P_{\mathrm{R}}}{b} \end{bmatrix} &= \widetilde{S}^{\infty}(a_0)\begin{bmatrix} \Delta_{\mathrm{V}} \\ \Delta_{\mathrm{H}} \\ b\Delta_{\mathrm{R}} \end{bmatrix} \\ &= \begin{bmatrix} S_{\mathrm{VV}}(a_0) & 0 & 0 \\ 0 & S_{\mathrm{HH}}(a_0) & S_{\mathrm{HR}}(a_0) \\ 0 & S_{\mathrm{RH}}(a_0) & S_{\mathrm{RR}}(a_0) \end{bmatrix}\begin{bmatrix} \Delta_{\mathrm{V}} \\ \Delta_{\mathrm{H}} \\ b\Delta_{\mathrm{R}} \end{bmatrix}.\end{aligned} \tag{24}$$

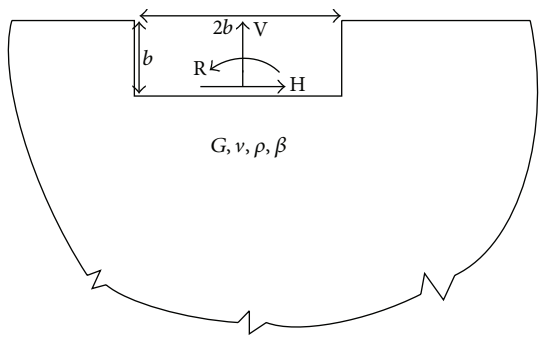

Figure 5: Cross section of a strip foundation embedded in a homogeneous half plane.

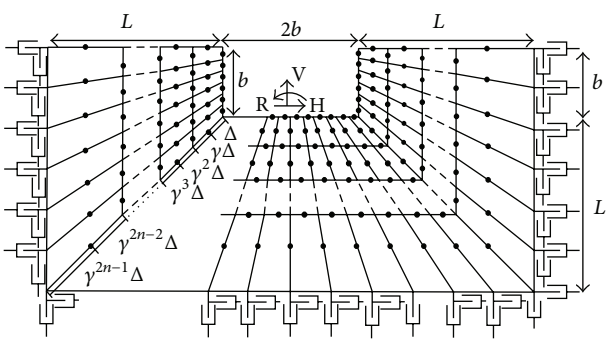

Figure 6: Finite element mesh of bounded medium.

The dynamic stiffness coefficients of the bounded medium are decomposed into the spring coefficient $k(a_0)$ and the damping coefficient $c(a_0)$:

$$S_{jj}(a_0) = \frac{1}{G}\left(k_{jj}(a_0) + ia_0 c_{jj}(a_0)\right) \quad j \in \{\mathrm{V}, \mathrm{H}, \mathrm{R}\}. \quad (25)$$

5.1.2. Numerical Evaluation. The discretization of the finite element mesh is shown in Figure 6, in which the eight-node isoparametric finite element is employed. The finer mesh is utilized near the strip foundation and it becomes coarser away from that with a proportionality factor γ. The material constants of the foundation are Poisson ratio $\nu = 0.25$ and natural damping ratio $\beta = 0.05$. The various initial conditions of the value optimization model and the corresponding optimum solutions of key factors are listed in Table 2. The dynamic stiffness coefficient solved by case C1 is seen as the accurate soil-structure interaction.

As the wave amplitude attenuation and the maximum finite element number in the bounded medium are held constant, the maximum of the difference function of the dynamic stiffness coefficient is a variable value. According to the comparison of the dynamic stiffness coefficient of cases C1, C2, C3, C4, and C5 shown in Figure 7, the smaller maximum of the difference function of the dynamic stiffness coefficient promotes the accuracy of the dimensionless dynamic stiffness coefficient of the unbounded medium.

As the maximum of the difference function of the dynamic stiffness coefficient and the maximum finite element number in the bounded medium remain unchangeable, the wave amplitude attenuation is a variable value. According to the comparison of the dynamic stiffness coefficient of cases C1, C6, C7, C8, and C9 shown in Figure 8, the larger wave amplitude attenuation improves the accuracy of the dimensionless dynamic stiffness coefficient of the unbounded medium.

As the maximum of the difference function of the dynamic stiffness coefficient and the wave amplitude attenuation are changeless, the maximum finite element number in the bounded medium is a variable value. According to the comparison of the dynamic stiffness coefficient of cases C1, C10, C11, C12, and C13 shown in Figure 9, the larger maximum finite element number reduces the computational efficiency but enhances the simulation precision of the dimensionless dynamic stiffness coefficient of the unbounded medium.

5.2. Verification in the Time Domain. A transient horizontal displacement is excited at the interface of the discretization of the finite element shown in Figure 10 to test the feasibility of the value optimization model of key factors in the time domain. The material constants of the medium are shear modular $G = 0.32\,\mathrm{GPa}$, Poisson's ratio $\nu = 0.25$, a density of $\rho = 2000\,\mathrm{kg/m^3}$, shear-wave velocity $c_s = 400\,\mathrm{m/s}$, dilatational wave velocity $c_p = 693\,\mathrm{m/s}$, and time step $\Delta t = 0.001\,\mathrm{s}$.

The transient excitation is a prescribed horizontal displacement at the center of the rigid base (with zero values for the vertical and rocking motions)

$$u_b(t) = \begin{cases} \dfrac{u_0}{2}\left[1 - \cos\left(2\pi\dfrac{t}{T}\right)\right] & 0 \le t \le 2T \\ 0 & t > 2T \end{cases} \quad (26)$$

with period $T = 8b/c_s$.

The initial conditions and the optimum solutions by the value optimization listed in Table 3 are realized by the damping solvent extraction method. The interaction force based on the case A1 is regarded as the exact interaction force of the foundation-structure.

Since the maximum finite element number in the bounded medium remains unchanged, the computational efficiency of the unbounded foundation-structure interaction is fixed. The interaction force shown in Figure 11 is calculated by the various initial conditions of the value optimization

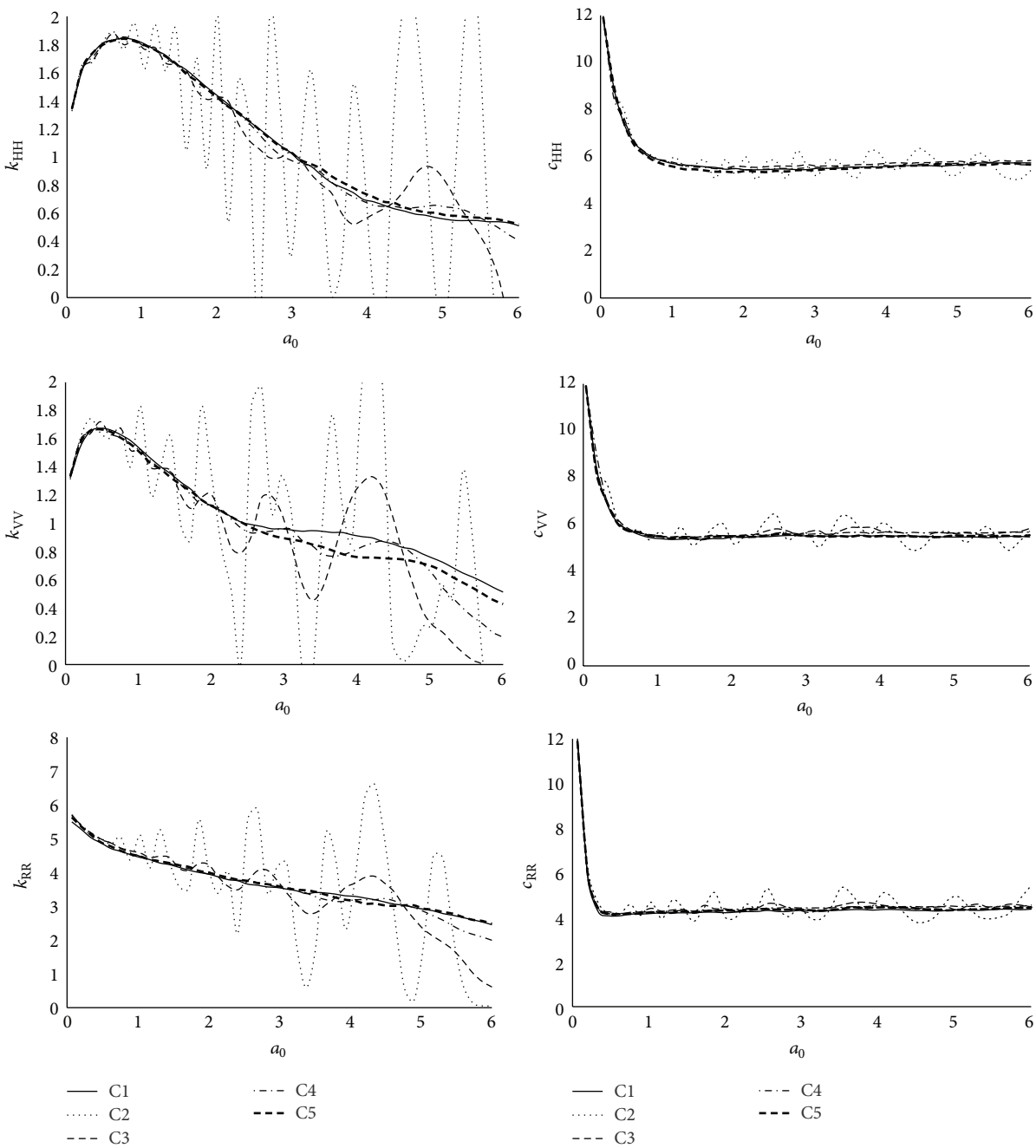

Figure 7: Effect of maximum of difference function of dynamic stiffness coefficient on dynamic stiffness coefficient.

model of key factors. When the maximum value of the difference function of the dynamic stiffness coefficients is a variable value (such as in cases A1, A2, A3, and A4), the larger wave amplitude attenuation improves the precision of the interaction force; nevertheless, the over-large attenuation has a negligible effect. When the wave amplitude attenuation is changeless (such as in cases A1, A3, A5, and A6), the smaller maximum of the difference function of the dynamic stiffness coefficient increases the accuracy of the soil-structure interaction force.

In summary, the implementation of the unbounded medium-structure interaction in the time-frequency domain illustrates that the alterable initial conditions of the value optimization model of key factors can improve the simulation accuracy and computational efficiency of the interaction, which are made up with the smaller maximum finite element number, the larger wave amplitude attenuation, and the smaller maximum of the difference function between the dimensionless dynamic stiffness coefficients of the damped and undamped unbounded foundation.

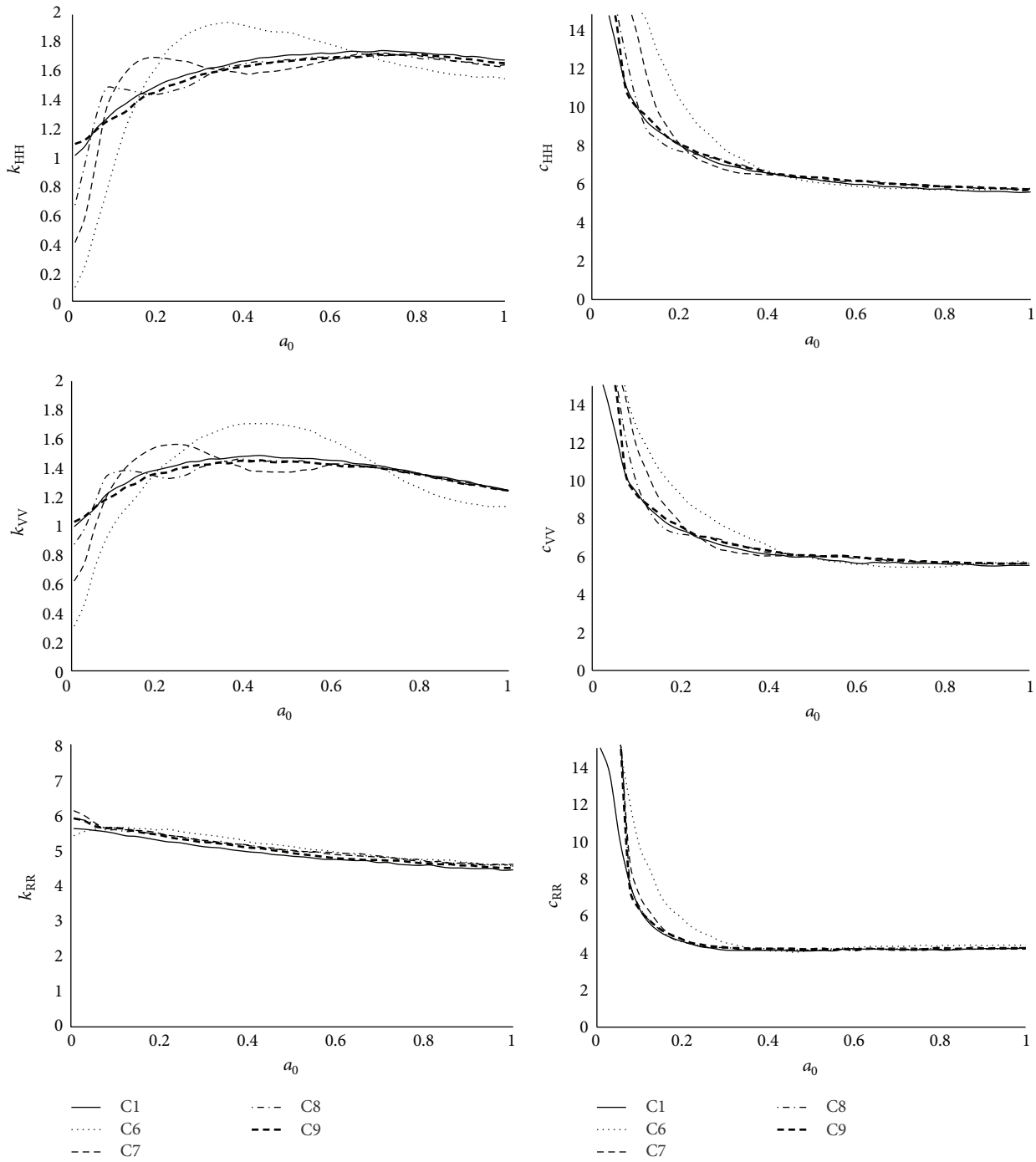

Figure 8: Effect of wave amplitude attenuation on dynamic stiffness coefficient.

6. Application

To demonstrate the adaptation of the value optimization model of key factors in practical engineering, the rock foundation-gravity dam shown in Figure 12 is applied to analyze the dynamic response of the dam to harmonic ground motion. The geometric properties of the gravity dam are the height, 132 m, and the width, which is 14 m at the crest and 110 m at the bottom. Taking the cross section of the medium-dam as an example, the dynamic response analysis of the gravity dam is calculated as a plane-strain problem. The material parameters of the gravity dam are Young's modulus of 20 GPa, Poisson's ratio of 0.18, and a density of 2600 kg/m^3. The material parameters of the rock foundation are Young's modulus of 2.4 GPa, Poisson's ratio of 0.333, a density of 2100 kg/m^3, and the characteristic length of 40 m. The constants of the displacement input harmonic wave are the amplitude, 0.2 m, and the cycle, 0.4 s. Meanwhile, the

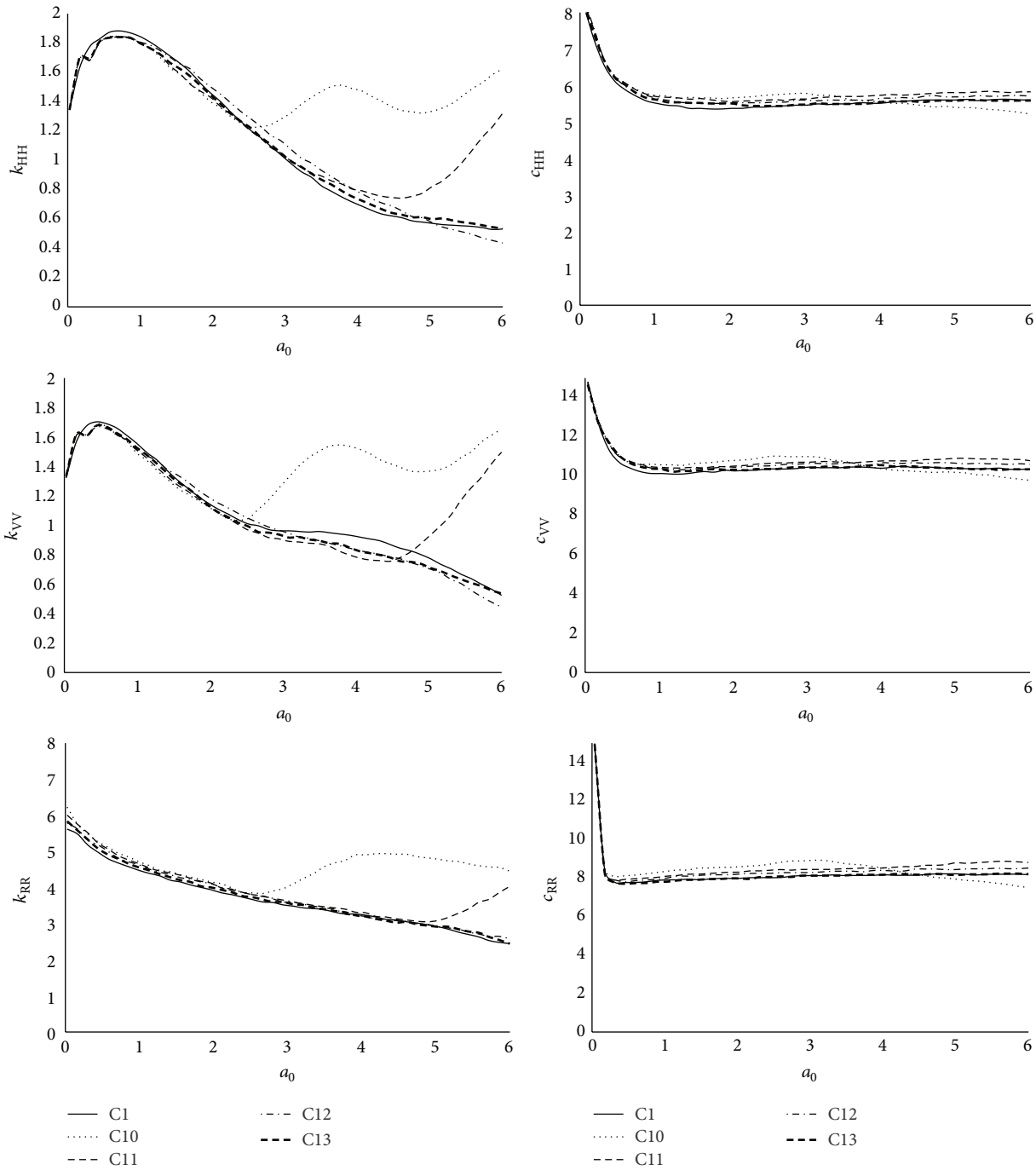

Figure 9: Effect of maximum finite element number on dynamic stiffness coefficient.

various initial conditions of the value optimization model of key factors based on the DSEM are implemented to analyze the dynamic response of the gravity dam.

The displacement function of the dam at the crest shown in Figure 13 indicates that the simulation precision and computational efficient of the displacement response of the gravity dam can be enhanced by reducing the maximum of the difference function of the dynamic stiffness coefficient and raising the wave amplitude attenuation at the interface and the maximum of finite element number in the bounded medium.

7. Conclusion

Considering the simulation accuracy and computational efficiency of the soil-structure interaction, this study's aim was to establish the value optimization model of key factors (such as the artificial damping ratio, the size of the bounded medium, and the finite element mesh density). From the impact assessment of the key factors on the dimensionless dynamic stiffness coefficient and the analysis of the interrelation among the key factors, the value optimization model of

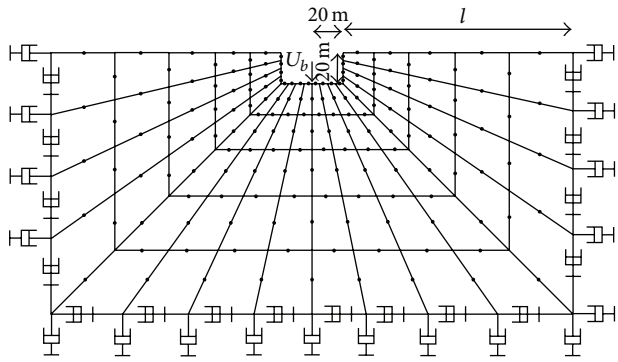

Figure 10: Finite element mesh of bounded media.

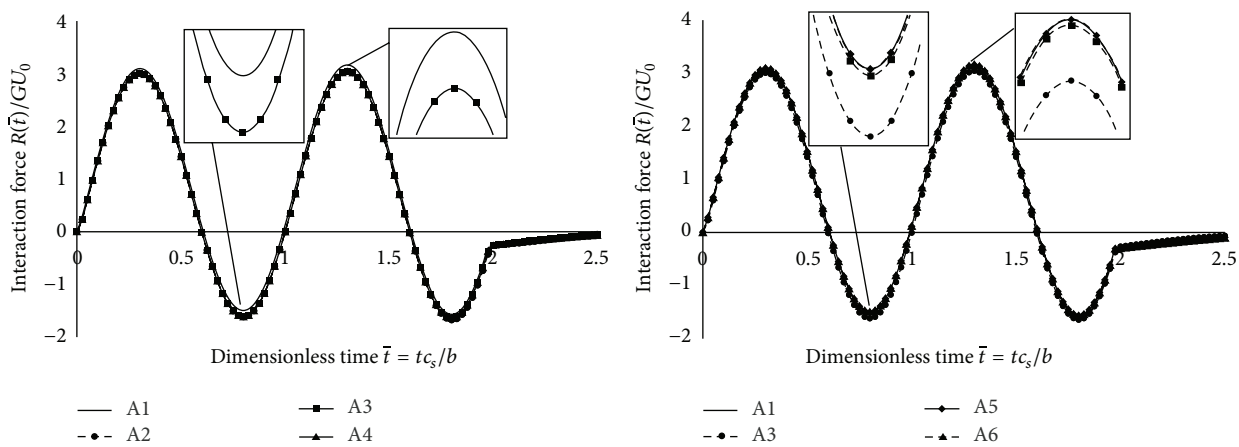

Figure 11: Time history of horizontal interaction force varying maximum of difference function of dynamic stiffness coefficient and wave amplitude attenuation.

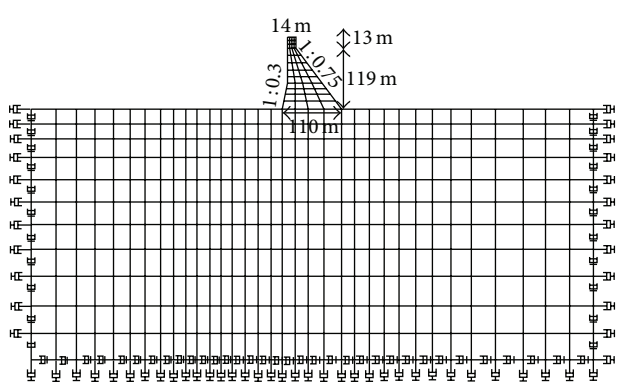

Figure 12: Finite element mesh of the gravity dam-bounded medium.

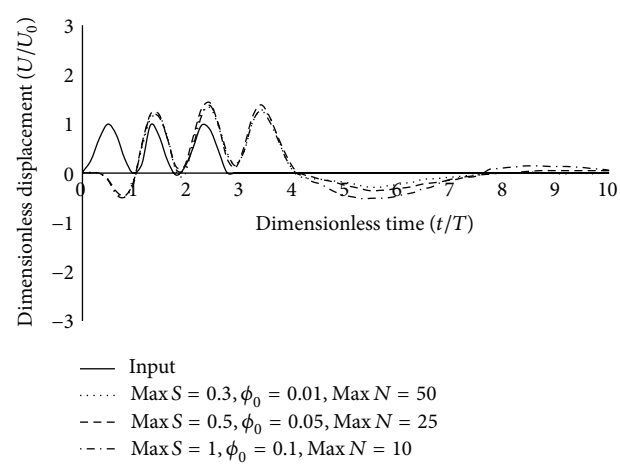

Figure 13: Dynamic magnification of crest displacements under seismic excitation $T = 0.4$ s.

key factors based on the DSEM was proposed. In additions, the initial conditions of the value optimization model were composed of the wave amplitude attenuation, the maximum finite element number, and the maximum of the difference function between the dimensionless dynamic stiffness coefficient of the undamped and damped unbounded medium.

The implementations of the dimensionless dynamic stiffness coefficient and the interaction force demonstrated that the value optimization model of key factors was capable of controlling the simulation accuracy and computational efficiency of the unbounded medium-structure interaction in the frequency and time domain. Finally, the displacement history function at the crest of the gravity dam on the rock foundation indicated that the value optimization model of key

Table 2: Characteristics of the finite element discretization of bounded medium.

Case	Initial condition			Optimal value of key factor				
	Max S	ϕ_0	Max N	$\bar{\zeta}$	l/b	n	Δ/b	γ
C1	0.32	0	2000	0.05	3000	2000	0.0028	1.002
C2	1.12	$1.00E-04$	25	0.6	7.68	25	0.062	1.044
C3	0.9	$1.00E-04$	25	0.4	11.51	25	0.074	1.052
C4	0.64	$1.00E-04$	25	0.2	23.03	25	0.094	1.066
C5	0.32	$1.00E-04$	25	0.1	46.06	25	0.114	1.080
C6	1.12	$1.00E-04$	25	0.6	7.68	25	0.062	1.044
C7	1.12	$1.00E-06$	25	0.6	11.51	25	0.074	1.052
C8	1.12	$1.00E-13$	25	0.6	24.95	25	0.096	1.068
C9	1.12	$1.00E-48$	25	0.6	46.06	25	0.114	1.095
C10	1.12	$1.00E-13$	6	0.6	23.03	6	0.429	1.304
C11	1.12	$1.00E-13$	12	0.6	23.03	12	0.201	1.142
C12	1.12	$1.00E-13$	18	0.6	23.03	18	0.131	1.093
C13	1.12	$1.00E-13$	25	0.6	23.03	25	0.094	1.066

Table 3: Various initial conditions and the optimum values of key factors.

Case	(Max S, ϕ_0, Max N)	$(l/b, \bar{\zeta}, n, \Delta/b, \gamma)_{\text{opt}}$
A1	(0.1, 0, 2000)	(3000, 0.05, 2000, 0.0028, 1.002)
A2	(1, 0.1, 25)	(2.4, 0.48, 25, 0.035, 1.025)
A3	(1, 0.05, 25)	(3.2, 0.48, 25, 0.044, 1.031)
A4	(1, 0.01, 25)	(4.8, 0.48, 25, 0.051, 1.036)
A5	(0.5, 0.05, 25)	(12.4, 0.12, 25, 0.075, 1.053)
A6	(0.3, 0.05, 25)	(37.4, 0.04, 25, 0.107, 1.076)

factors based on the DSEM was appropriate for analyzing the interaction of the practical unbounded medium-structure.

Competing Interests

The authors declare that there is no conflict of interests regarding the publication of this paper.

Acknowledgments

This work was supported by National Natural Science Foundation of China (51279053).

References

[1] J. Lysmer and G. Waas, "Shear waves in plane infinite structures," *Journal of the Engineering Mechanics Division*, vol. 98, no. 1, pp. 85–105, 1972.

[2] Z. P. Liao and H. L. Wong, "A transmitting boundary for the numerical simulation of elastic wave propagation," *International Journal of Soil Dynamics and Earthquake Engineering*, vol. 3, no. 4, pp. 174–183, 1984.

[3] S. Chongmin and Z. Chuhan, "A dynamic boundary element method for earthquake resistant analysis of dams," *Earthquake Engineering & Engineering Vibration*, vol. 8, no. 4, pp. 14–25, 1988.

[4] C. Song and J. P. Wolf, "Dynamic stiffness of unbounded medium based on damping-solvent extraction," *Earthquake Engineering & Structural Dynamics*, vol. 23, no. 2, pp. 169–181, 1994.

[5] J. P. Wolf and C. Song, *Finite-Element Modeling of Unbounded Media*, John Wiley & Sons, Chichester, UK, 1996.

[6] J. Chen, J. Li, and J. Zhou, "Seismic analysis of large 3-D underground caverns based on high performance recursive method," *International Journal of Solids and Structures*, vol. 41, no. 11-12, pp. 3081–3094, 2004.

[7] J.-B. Li, J.-Y. Chen, and G. Lin, "Finite element damping-extraction method for dynamic interaction time domain analysis of non-homogeneous unbounded rock," *Chinese Journal of Geotechnical Engineering*, vol. 26, no. 2, pp. 263–267, 2004.

[8] J.-Y. Chen, J. Li, and J.-B. Li, "A refined sub-regional reciprocal method in time domain and its application in dynamic interaction analysis," in *Proceedings of the 13th World Conference on Earthquake Engineering*, Vancouver, Canada, August 2004.

[9] J. B. Li, J. Yang, and G. Lin, "A stepwise damping-solvent extraction method for large-scale dynamic soil-structure interaction analysis in time domain," *International Journal for Numerical and Analytical Methods in Geomechanics*, vol. 32, no. 4, pp. 415–436, 2008.

[10] Y. Chen, X. Wang, and X. Zhou, "Time domain damping-extraction method for interaction of unbounded media with fractional-order," *Chinese Journal of Rock Mechanics and Engineering*, vol. 28, supplement 2, pp. 3666–3672, 2009.

[11] H. Zhong, G. Lin, J. Li, and J. Chen, "An efficient time-domain damping solvent extraction algorithm and its application to arch dam-foundation interaction analysis," *Communications in Numerical Methods in Engineering with Biomedical Applications*, vol. 24, no. 9, pp. 727–748, 2008.

[12] Y.-H. Chen, X.-Q. Wang, X.-D. Zhou, and Y.-D. Gui, "Determination of impact of pile driving vibration on seawall by infinite foundation method," *Journal of Hydraulic Engineering*, vol. 42, no. 2, pp. 226–231, 2011.

[13] M. A. Xiuping, *The DSE Method in Time-Domain of Dynamic Interaction Analysis*, Dalian University of Technology, Dalian, China, 2006.

[14] Y. Xunqiang, L. Jianbo, W. Chenglin, and L. Gao, "ANSYS implementation of damping solvent stepwise extraction method for nonlinear seismic analysis of large 3-D structures," *Soil Dynamics and Earthquake Engineering*, vol. 44, pp. 139–152, 2013.

[15] E. A. Kausel, "Complex frequencies in elastodynamics, with application to the damping-solvent extraction method," *Journal of Engineering Mechanics*, vol. 136, no. 5, pp. 641–652, 2010.

[16] H.-P. Ding and Z.-P. Liao, "Improvement of dynamic stiffness calculation based on damping-solvent extraction method," *Earthquake Engineering & Engineering Vibration*, vol. 21, no. 2, pp. 13–18, 2001.

[17] M. R. Hajiabadi and V. Lotfi, "An effective approach for utilizing damping solvent extraction method in frequency domain," *Soil Dynamics & Earthquake Engineering*, vol. 38, pp. 46–57, 2012.

[18] U. Basu and A. K. Chopra, "Numerical evaluation of the damping-solvent extraction method in the frequency domain," *Earthquake Engineering & Structural Dynamics*, vol. 31, no. 6, pp. 1231–1250, 2002.

[19] Y. Xun-Qiang, *Improvement and Engineering Application of Structure-Foundation Dynamic Interaction Model*, Dalian University of Technology, 2013.